Journal of Food Composition and Analysis 125 (2024) 105809

Contents lists available at ScienceDirect

Journal of Food Composition and Analysis

journal homepage: www.elsevier.com/locate/jfca

In situ screening of sodium sulfite residue on edible mushroom using SERS active paper swab

Shiyao Wang [a,b,1], Yanan Zhao [a,b,1], Chaofan Zhang [a,b], Shuai Cui [a,b], Liangxiao Zhang [c,*], Yisheng Chen [a,b,**]

[a] College of Food Science and Engineering, Shanxi Agricultural University, Taigu 030801, Shanxi, China
[b] Food Nutrition and Safety Institute, Shanxi Agricultural University, Taiyuan 030031, Shanxi, China
[c] Key Laboratory of Biology and Genetic Improvement of Oil Crops, Ministry of Agriculture and Rural Affairs; Laboratory of Risk Assessment for Oilseed Products (Wuhan), Ministry of Agriculture and Rural Affairs; Quality Inspection and Test Center for Oilseed Products, Ministry of Agriculture and Rural Affairs; Oil Crops Research Institute, Chinese Academy of Agricultural Sciences, Wuhan 430062, China

ARTICLE INFO

Keywords:
Sodium sulfite
SERS
Printing paper
AgNPs
Edible mushroom

ABSTRACT

In the present study, a printing paper functionalized with Ag nanoparticles (AgNPs) was used as a flexible surface-enhanced Raman spectroscopy (SERS) swab (AgNP@FP) to evaluate its ability to detect sodium sulfite residues on the surface of edible mushrooms. The results showed that the prepared AgNP@FP swab had fingerprint-like signals (at 620 and 927 cm^{-1}), which could serve as a clear confirmation of the analyte. In addition, the swab not only exhibited good repeatability, with spot-to-spot variation of < 2.6% at 620 cm^{-1} signal intensity, but it also met the requirement of commercial transportation as the peak intensity at 620 cm^{-1} remained at 57.84% of its initial value after 5 days of storage. The sensitivity of the substrate to sodium sulfite on the surface of oyster mushroom and enoki mushroom was as low as 0.2 mg/mL. The limit of detection (LOD) values of the sulfite residue on the surface of oyster and enoki mushrooms were 1.2 and 1.6 mg/kg, respectively. This study demonstrated that the AgNP@FP swab provided a simple tool for obscure and in situ screening of residues on the surface of agricultural products.

1. Introduction

Additives are used in foods to maintain their color, taste, and other qualities (Yang et al., 2022a; 2022b; 2020). As a food additive, sodium sulfite is frequently used to preserve fresh fruits and vegetables (Qu et al., 2017), prevent discoloration of glazed fruits and dried vegetables, and protect against bacterial contamination and oxidation during wine-making (Liu et al., 2021a; 2021b; Robbins et al., 2015). In the human body, sodium sulfite reacts with water to form bisulfite ions, sulfite ions, and SO_2 (Devarajan et al., 2023), which could further react with various body fluids and cellular components (Oshimo et al., 2021). Sulfite has multifaceted toxic effects. Excessive or high concentrations of SO_2 and its derivatives can damage body organs (Li et al., 2022). For example, SO_2 not only degrades vitamin B_1 and adversely affects body growth, causing polyneuritis (Zhang et al., 2016), but it also causes intestinal dysfunction, leading to diarrhea, headache, and liver damage and impairing the health and function of the digestive system (Chen et al., 2015a; 2015b; Lester, 1995). SO_2 also induces respiratory diseases (Han et al., 2020; Wang et al., 2016)) such as asthma, rhinitis, bronchitis, and lung cancer as well as impairs the cardiovascular and nervous systems (Yao et al., 2015; Yao et al., 2016). In this context, the Joint FAO-WHO Expert Committee on Food Additives (Gonçalves et al., 2020; Irwin et al., 2017; Lajin and Goessler, 2019) stipulated 0.7 mg/kg as an acceptable daily intake (ADI) limit of sodium sulfite (equal to SO_2) per person. Therefore, it is crucial to regulate the amount of sodium sulfite used as an additive for edible mushrooms.

Currently, the main methods to detect sulfites include gas chromatography-mass spectrometry (Carrascon et al., 2017), high-performance liquid chromatography (Urupina et al., 2020), liquid chromatography-tandem mass spectrometry (Carlos and de Jager, 2017), and fluorescence analysis (L. Wang and Chen, 2020). However, these technologies have several limitations, such as time-consuming

* Corresponding author.
** Corresponding author at: College of Food Science and Engineering, Shanxi Agricultural University, Taigu 030801, Shanxi, China.
E-mail addresses: zhanglx@caas.cn (L. Zhang), chenyisheng@sxau.edu.cn (Y. Chen).
[1] Shiyao Wang and Yanan Zhao contributed equally to this work.

https://doi.org/10.1016/j.jfca.2023.105809
Received 10 June 2023; Received in revised form 26 September 2023; Accepted 1 November 2023
Available online 4 November 2023
0889-1575/© 2023 Elsevier Inc. All rights reserved.

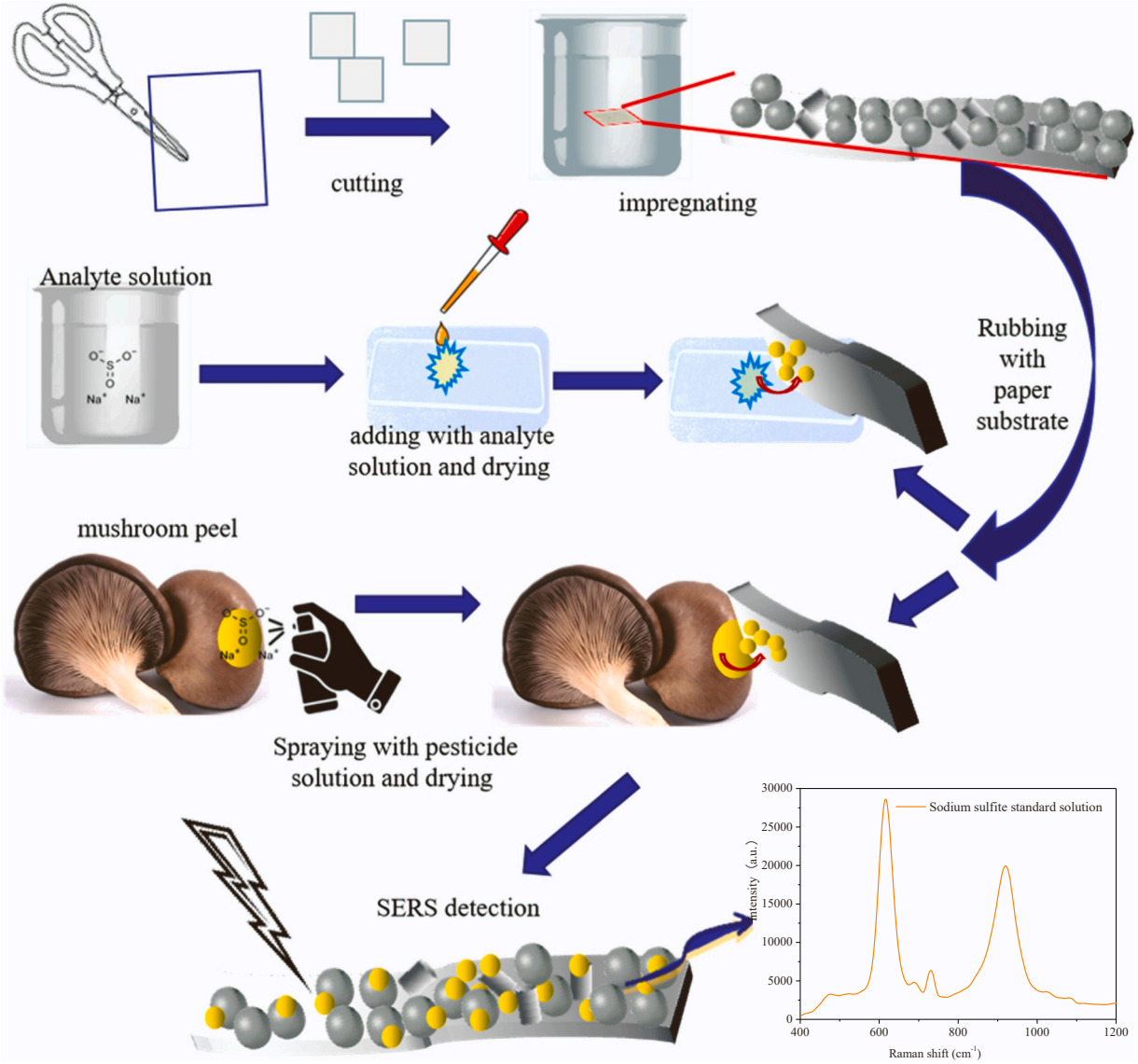


Fig. 1. Flow chart of SERS detection.

process, complex sample preparation, high demand for personnel and specialized equipment, and poor sensitivity and selectivity (Yang et al., 2021a; 2021b; 2022a). Therefore, faster, simpler, and more accessible detection methods are required.

Surface-enhanced Raman spectroscopy (SERS) is an efficient, universal, and unlabeled molecular fingerprinting technique that is widely used to detect trace substances (Li et al., 2022a; Yang et al., 2023a; 2023b). Raman scattering is a phenomenon involving inelastic scattering between laser photons and molecules (the excitation of molecular vibration causes the energy of scattered photons to be typically lower than that of incident photons), which produces the Raman spectrum, thereby providing structural information about the sample. Electromagnetic wave enhancement is associated with local surface plasmon resonance and chemical enhancement induced by charge transfer to the adjacent noble metal nanostructure and forms the principle underlying Raman enhancement (Shang et al., 2017). The application of SERS depends on the development of its substrate, leading to the continuous improvement of its substrate structure. The traditional Raman substrate was developed based on the deposition of nanoparticles of noble metals such as Au, Ag, and Cu on rigid substrates such as glass slides and silicon wafers (Shariat, 2023; Weng et al., 2019). However, the substrate was difficult to adapt to the requirement of nondestructive testing as it required complex pretreatment to detect solid samples on a nonplanar surface. Flexible materials, including substrates (Khan et al., 2022), adhesive tape (Bai et al.,2023), textile materials (Gao et al., 2020), and hydrophobic materials (Zhang et al.,2019), could be attached effectively on the curved surface, which can provide portability (Batool et al., 2022; Chen et al., 2017). Thus, flexible SERS substrates have significant advantages over traditional substrates. Flexible SERS substrates can be cut into any desired shape and size for on-demand use. Moreover, these substrates have high porosity, low preparation cost, flexibility, and folding and bending ability (Liu et al., 2021a; 2021b; Tian et al., 2021; Zheng et al., 2021). Compared to rigid SERS substrates, flexible substrates have significant advantages in the extraction, filtration, and concentration of probe molecules in complex samples.

In SERS detection, the Raman signals of molecules can be effectively enhanced only if the distance between the molecule of the analyte and the surface of the SERS substrate is sufficiently close. As the distance increases, the Raman enhancement effect of the molecule decreases exponentially (Fang et al., 2015; Lin and He, 2019; Pang et al., 2016). Raman “hot spots” are areas where Raman signals can be significantly enhanced; these spots typically appear at sharp edges or small gaps in the tightly arranged nanoscale plasma nanostructure (Cialla et al., 2012; Mandal and Tewari, 2022). Printing paper is a common commodity in

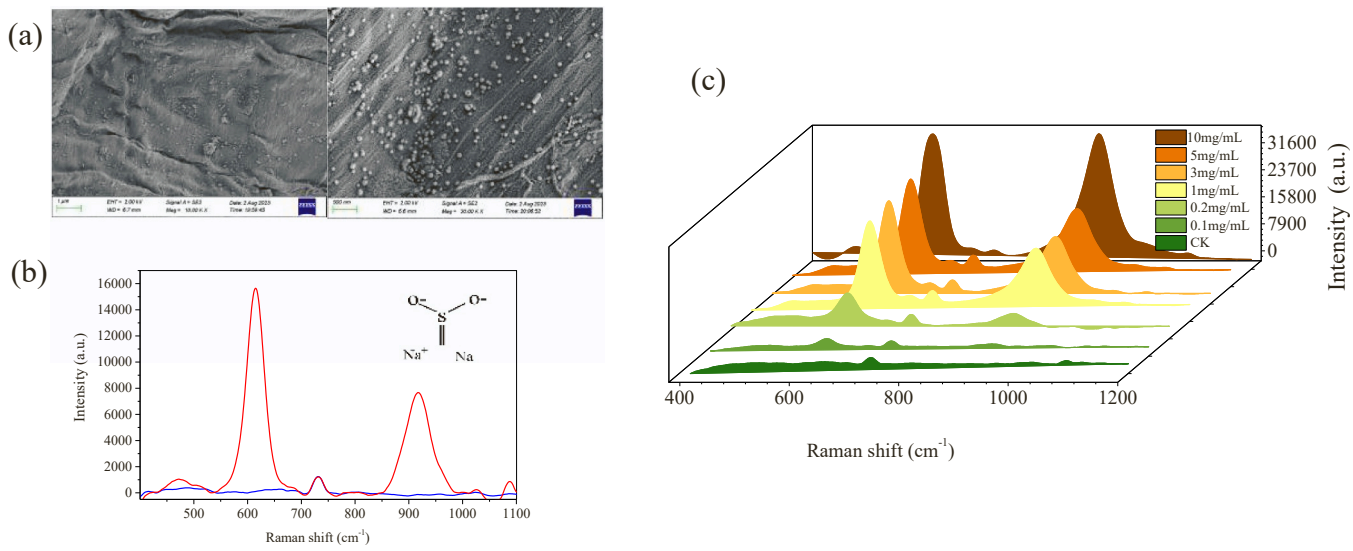


Fig. 2. (a) SEM of the AgNP@FP swab; (b)Measurement and molecular formula of sodium sulfite; (c) SERS sensitivity after substrate wiping of the glass plate.

daily life. A flexible SERS substrate based on printing papers can be both practical and cost-effective. Because of the compact fiber structure of the printing paper, the liquid could remain on its surface through immersion for a longer time. Moreover, this structure can enable reduced silver to easily come in contact with the test molecule, thereby achieving effective enhancement of Raman signals.

Therefore, in the present study, the SERS detection technology was used for sulfite detection on the surface of mushrooms. Printing paper was chosen as the substrate in this experiment, and a sodium sulfite standard solution was dropped on the surface of mushrooms to test its usage, as shown in Fig. 1. The sensitivity, uniformity, and stability of the prepared SERS substrate were analyzed. AgNP@FP was used to detect the presence of sulfite on mushroom surface and to explore the relationship between its concentration and the SERS peak intensity.

2. Materials and methods

2.1. Materials and methods

Silver nitrate ($AgNO_3$ ≥99.8%), sodium citrate ($C_6H_5Na_3O_7 \cdot 2\ H_2O$ ≥99%), ultrapure water (conductivity: 1.08 μS/cm), oyster mushroom, and enoki mushroom were purchased from a local supermarket (Taiyuan, China). A4-size printing papers and sodium sulfite were bought from Sinopharm Chemical Reagent Co., Ltd. (Beijing, China). The specification of the A4-size printing paper (defined by ISO 216 issued by the International Organization for Standardization) was 21 cm × 29.7 cm. A magnetic heating stirrer (MS-H-ProA, Dragon Laboratory Instruments Ltd.), a portable Raman spectrum analyzer (ATR3110, Optosky (Xiamen) Photonics Inc.), and a scanning electron microscope (Gemini SEM 300) were used for the experiment.

2.2. Sample preparations

Pretreatment of the sample: the purchased fresh oyster mushroom and enoki mushroom were rinsed, and their surfaces were dried with the printing paper. Preparation of nano-Ag colloid: silver nitrate (45.0 mg) was dissolved in ultrapure water (250 mL), stirred evenly, and heated to boiling. Next, 1% trisodium citrate solution (5 mL) was constantly added dropwise to the abovementioned solution. The solution was boiled for 1 h, removed from the heater, and stirred constantly until it reached room temperature. This resulted in a grey-green nano-Ag colloid, which was sealed and stored in the dark at 4 °C (Lee and Meisel, 1982; Shi et al., 2016). Preparation of the flexible substrate: the clean printing paper was cut into a substrate (1 cm × 1 cm) and placed over the prepared nano-silver colloid. After the AgNPs were evenly adsorbed on the substrate, the substrate was taken out, dried, and sealed for further use. Preparation of sodium sulfite standard solution: sodium sulfite powder (0.05 g) was dissolved in ultrapure water (5 mL) in a centrifuge tube to prepare the sodium sulfite standard solution (10 mg/mL). This solution was further diluted to prepare standard solutions of 5, 3, 1, 0.2, and 0.1 mg/mL; these solutions were shaken well and kept aside for further analysis.

2.3. Detection conditions and methods

Detection condition of SERS: A portable Raman spectrometer was used for the experiment in a clean and tidy laboratory. The parameters were set as follows: excitation wavelength, 785 nm; laser power, 80 mW; sampling interval, 500 ms; integration time, 8000 ms; average frequency, 1; signal-to-noise ratio threshold, 3; intensity threshold, 1000.

Detection method of sensitivity: the sample standard solutions (10 μL) at different concentrations were dropped on clean glass plates. After the plate was dried, it was wiped with the soaked printing paper substrate, and SERS detection was then performed. The blank group was the prepared flexible substrate for wiping the glass plate.

Detection method of uniformity: SERS detection was performed at 20 random points on an AgNP@FP swab. A standard sodium sulfite solution (1 mg/mL) was used for the test. The testing method was the same as mentioned above.

Detection method of stability: five AgNP@FP swabs were placed in sealed glass plates and stored in a dark place (18 °C, 30–50% humidity). SERS was performed daily with a standard sodium sulfite solution for 5 days.

Detection of sample: sodium sulfite standard solutions at different concentrations were dropped on the surface of the washed mushroom sample. After natural drying, the prepared ethanol-water solution (1:1 ratio) was sprayed on the sample, and SERS was then performed. To confirm that the purchased mushrooms did not contain sulfite, we performed SERS on the washed mushrooms and used them as a blank control group.

2.4. Data analysis and processing

NGSLABSPEC software (Oppo Tiancheng Corporation) was used for spectral data pretreatment and baseline processing of the Raman

Table 1
The principal characteristic peaks in sodium sulfite Raman spectra and their distribution.

Characteristic peak (cm^{-1})	Intensity	Signal ascription
620	Strong	attributed to the symmetric bending vibration of O-S-O.
927	Intermediate	attributed to the symmetric and asymmetric stretching vibration of S-O stretching vibration.

spectra. Origin 8.5 software (OriginLab) was used to analyze the collected data and draw maps. ChemDraw 20.0 (Revvity Signals Software) was used to draw the required chemical formula. Each sample was analyzed three times, and the average value was taken as the final value.

3. Results and discussion

3.1. Assessment of sensitivity

The characteristic details of the AgNP@FP swab are shown in Fig. 2 (a). AgNPs were widely and evenly distributed on the printing paper. They were spherical particles (rod-shaped particles occasionally) with a radius of approximately 100 nm. This type of structure was beneficial for forming an effective "hotspot." The Raman spectra of the sodium sulfite aqueous solution was first determined. As shown in Fig. 2(b), two characteristic peaks were detected at 927 and 620 cm^{-1}, which was consistent with previous findings (Chen, et al.,2016). The characteristic peak attributions are listed in Table 1. However, no characteristic diffraction peak of sodium sulfite was noted in the blank sample; this finding indicated that the prepared AgNP@FP swab could be used to detect sodium sulfite. Because of the chemical affinity between S and Ag, S-O stretching (symmetry+symmetry), and O-S-O symmetry, SO_2 was bound to the surface of AgNPs, thereby generating two strong and comparable characteristic peaks at 927 and 620 cm^{-1}. Relative deviations in the characteristic peak were noted under the condition of variable strength of the S-O tensile band (Deng et al.,2015; Huang et al., 2017). The sensitivity was then investigated by dropping sodium sulfite standard solution (10 μL) on the glass plate. The plate was dried and wiped with the printing paper substrate and analyzed by Raman spectroscopy. As shown in Fig. 2(b), the characteristic peak at 620 cm^{-1} could be clearly distinguished at a concentration as low as 0.1 mg/mL, while the peak at 927 cm^{-1} disappeared. Hence, we performed a quantitative analysis of the 620 cm^{-1} peak, establishing a standard curve correlating sample concentration and peak intensity. As illustrated in Fig. S1, the concentration range of the sodium sulfite standard solution spanned from 0.1 to 10 mg/mL. The standard curve for the sodium sulfite standard solution ($y = 4678.2x+20620.7$, $R^2 = 0.991$) exhibited excellent linearity. This observation suggested that the flexible substrate, represented by the printing paper, possessed high sensitivity in detecting sodium sulfite, likely attributable to its relatively compact fiber structure. The impregnation process ensured prolonged liquid retention on the printing paper's surface, enhancing electrostatic interactions among silver ions and resulting in a dense and uniform structure. Consequently, sodium sulfite molecules were more prone to contact reduced silver, leading to an amplification of Raman signals.

The enhancement factor (EF) is a key indicator that represents the enhancement magnitude in SERS detection. Fig. S2 shows the SERS spectrum of 10^{-1} mg/mL sodium sulfite and the Raman spectrum of 10 mg/mL sodium sulfite adsorbed on the AgNP@FP swab. The EF value (3.68×10^4) was calculated with the 620 cm^{-1} peak as a reference. The details of the relevant calculations are provided in Supporting Information.

3.2. Assessment of uniformity and stability

The uniformity of the printing paper substrate was investigated with the sodium sulfite solution (1 mg/mL) as the probe through wiping, as shown in Fig. 3. The repeatability of varying locations was assessed for one AgNP@FP swab through multiple measurements (20 times) at stochastically chosen locations on a single SERS swab (Fig. 3(a)). The SERS spectral results for the 20 measurements are shown in Fig. 3(c-e). As shown in Fig. 3(b), no significant change was noted in the characteristic peak intensity at 620 and 927 cm^{-1}, with a relative standard deviation (RSD) of 2.6%. The SERS signal display rate reached 100% in 20 detections, thus indicating that the sample was evenly distributed on the substrate. As shown in Fig. 3(c), the intensity exhibited no significant change in the SERS response peak at 620 cm^{-1} for the 20 points, thus indicating a good uniformity in the distribution of AgNPs on the printing paper. The experimental result confirmed the superiority of the printing paper as a flexible substrate. Similarly, to test the stability of the test strips, the same batch of the soaked substrate was used for analysis. Fig. 4 shows the results of the stability analysis for 5 days. The stability of the swab gradually decreased over time. On the fifth day, the characteristic peaks at 620 and 927 cm^{-1} remained clear and easily distinguishable, with a peak intensity of approximately 50% as compared to that on the first day. Because AgNPs were fixed on the printing paper by soaking, they were mostly attached to the surface of the printing paper; this made AgNPs prone to oxidation and other phenomena, thereby resulting in the loss of the "hotspot." Thus, the stability of swab decreased over time. However, the retention value met the detection requirement in 5 days, which provided the possibility of commercial

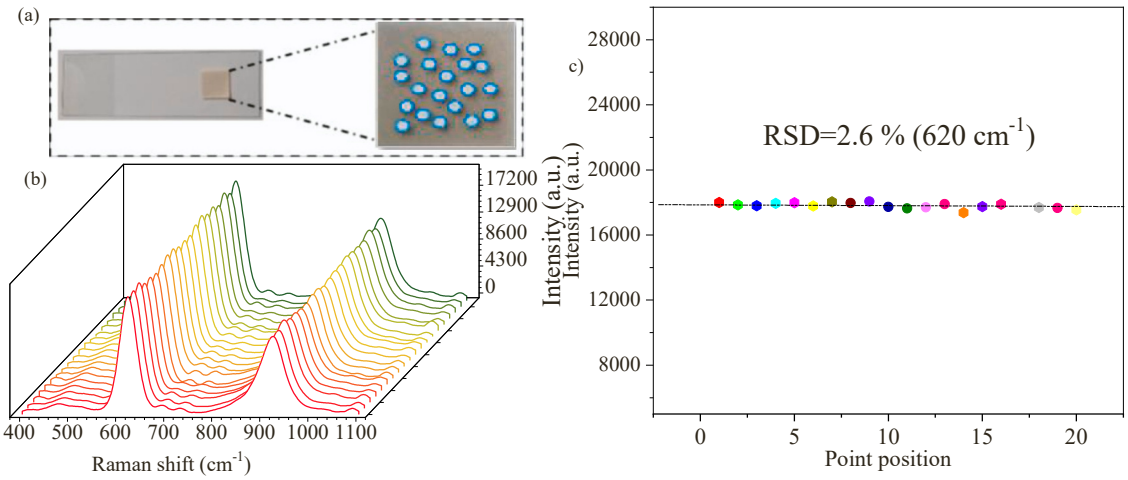


Fig. 3. (a) Schematic plot of the random 20 points of a single substrate; (b) Random 20-point spectrogram of a single substrate; (c) Random 20-point scatter map.

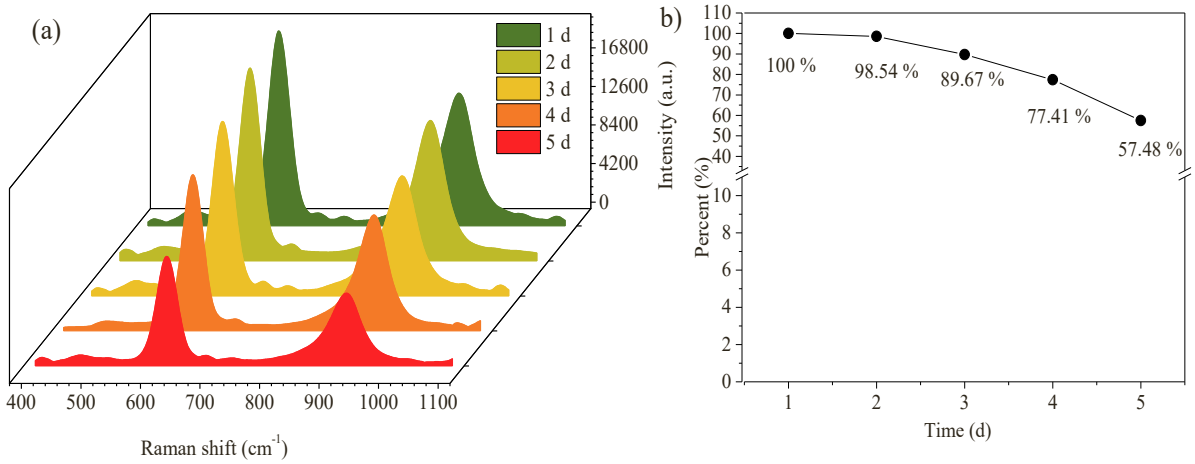


Fig. 4. (a) Test diagram of 5-day stability; (b) The stability of the 620 cm^{-1} peak intensity over 5 days.

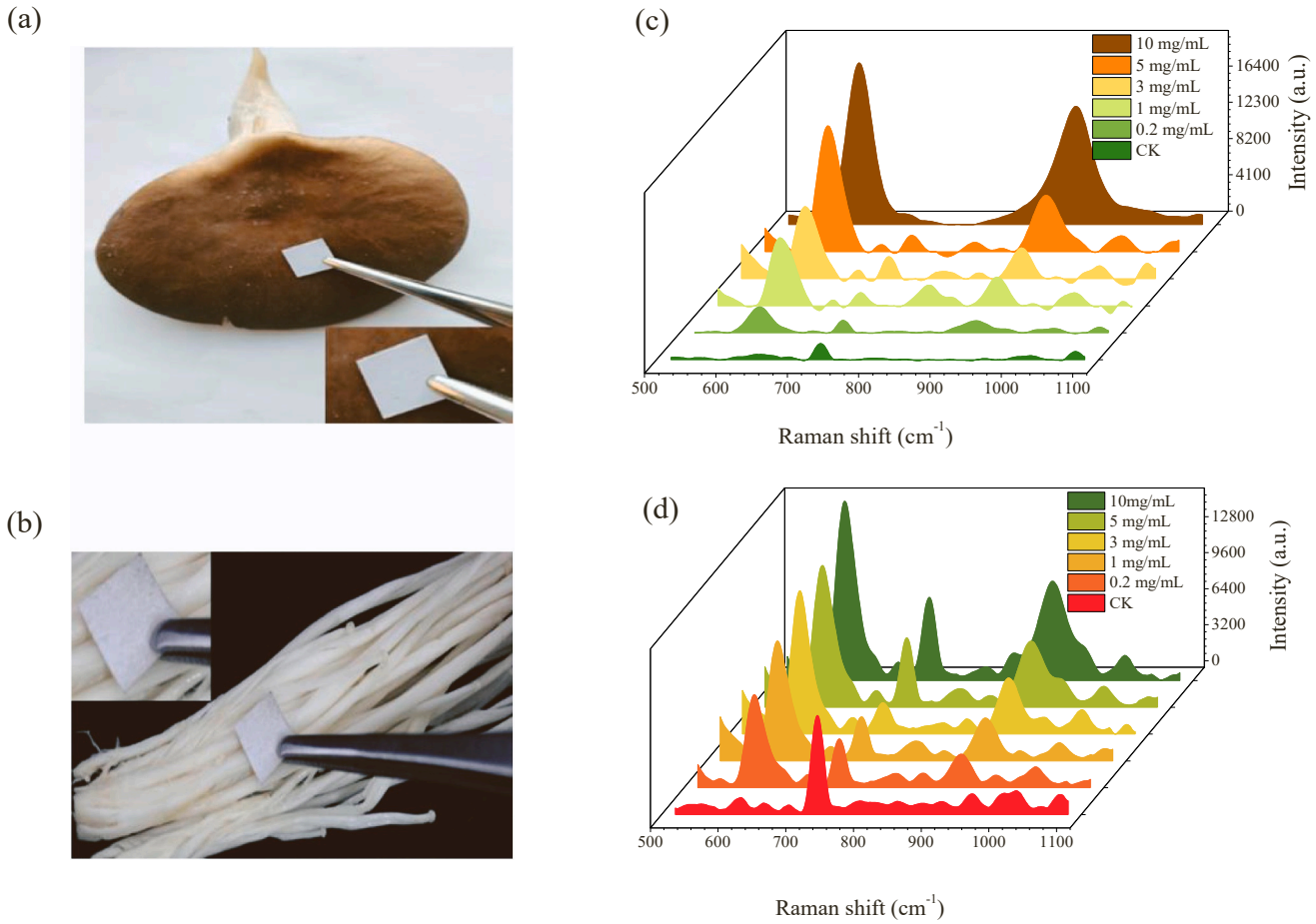


Fig. 5. (a, b) Diagram of the surface wiping of oyster mushrooms and enoki mushrooms; (c, d) SERS sensitivity diagram of oyster mushrooms and enoki mushrooms.

transportation.

3.3. Detection of sodium sulfite in edible mushrooms

Fig. S3 shows a comparison of a blank sample to a standard sodium sulfite solution without sodium sulfite residue on the mushroom surface. The results of the SERS analysis of oyster mushrooms and enoki mushroom wiped with sodium sulfite standard solutions at different concentrations are shown **in** Fig. 5(a) and (b). The surfaces of the mushrooms were dried, and sodium sulfite standard solutions at different concentrations were applied to their surfaces. After the solutions were fully absorbed by the fungus, the standard ethanol aqueous solution was sprayed on the area where the solution was added for wetting. Subsequently, the soaked printing paper substrate was picked up with a tweezer and wiped at the place to be measured so that the solution was in fully contact with the substrate. SERS detection was performed when the substrate was dried. The detection result of the edible mushrooms is shown in the two small figures (c) and (d) in Fig. 5.

Table 2
SERS detection of sulfites.

Method	Analyte	Food matrix	LOD	Reference
NIR-HSI+NIR	Sodium metabisulfite	Fresh-cut potatoes	0.5 mg/kg	(Bai et al., 2020)
Electrochemical alloying/dealloying sensor	Sulfite	Canadian Beef	47.43–60.26 mg/kg	(Manikandan et al., 2018)
ICT-ratiometric fluorescent probe	Sulfite	Chinese yam	3.01 mg/kg	(Lan et al., 2022)
PRA-optical sensor	Sulfite	Apricot	1.23 ± 0.04 mg/kg	(Bener et al., 2020)
HS-TFME+SERS	Sulfite	Herbs	6 mg/kg	(Dong et al., 2019)
SERS	Sulfite	Fungus	1.2 mg/kg	In this work

Abbreviations: Near-infrared hyperspectral imaging (NIR-HSI) system and portable near-infrared (NIR) spectrometer. Intramolecular charge transfer ratiometric fluorescent probe (ICT-ratiometric fluorescent probe). Pararosaniline -optical sensor (PRA-optical sensor) Headspace thin-film microextraction (HS-TFME)

With the decrease in sodium sulfite concentration, the 620 and 927 cm^{-1} SERS intensity peaks were reduced. Because of the influence of mushroom on the substrate, its sodium sulfite detection limit reached only 0.2 mg/mL. Finally, quantitative analysis was conducted using the SERS characteristic peak to determine the standard curve of the sample concentration and the characteristic peak intensity at 620 cm^{-1}. As shown in Fig. S4 (a, b), the standard curve for surface-enhanced Raman scattering of oyster mushroom was $y = 2490.7\ lgc + 7766.3$ ($R^2 = 0.989$), while that for enoki mushroom was $y = 1534.5\ lgc + 9980.2$ ($R^2 = 0.991$). The limit of detection (LOD) was calculated based on the average of the corresponding background peaks generated from a blank substrate (10 experiments) plus 3 times the standard deviation. The LODs of the printing paper used as the flexible substrate for detecting sodium sulfite in oyster and enoki mushrooms were 1.2 and 1.6 mg/kg, respectively; these values were far lower than the Chinese national standard of 0.05 g/kg. Compared to the results of SERS detection of sulfite reported in recent years, our detection method was simpler and more economical, as shown in Table 2. The most common office printing paper was used as a substrate, and the simplest immersion method was adopted to transfer AgNPs on its surface. The preparation of AgNPs was simple, and the entire process was rapid. The experiment also confirmed that the flexible SERS substrate with the printing paper as the substrate had high sensitivity and good uniformity, particularly for detecting pesticide residues on the surface of mushroom. However, there were some disadvantages, according to previous literature, such as the complex synthesis process of nanoparticles, difficult substrate preparation, stringent requirement for operators, and relatively difficult detection process. Bai et al. (2020) utilized a near-infrared hyperspectral imaging (NIR-HSI) system along with a portable NIR spectrometer for the identification of sulfur dioxide residues on freshly cut potato chips immersed in sodium metabisulfite solutions of varying concentrations. The inspection procedure encompassed tasks such as cleaning, slicing, and submerging whole purchased potatoes into distinct pyrosulfite standard solutions. Additionally, it involved the setup, parameter configuration, and calibration of the NIR-HSI system. Manikandan and co-authors (Manikandan et al., 2018) synthesized nanoporous gold through the chemical etching of gold-silver alloys to create 3D nanoporous gold microelectrodes. These nanoporous gold microelectrodes were subsequently employed for the detection of nitrite in beef. Dong et al. (2019) developed a detection approach employing headspace thin film microextraction (HS-TFME) in conjunction with surface-enhanced Raman spectroscopy (SERS). They deposited sea urchin-like ZnO micron particles onto glass plates using the chemical liquid deposition method and applied them in the analysis of Chinese herbal sulfites. These three methods are limited due to the precision and cost of the testing instruments; consequently, the technical requirements for the testing personnel are higher. Moreover, these methods involve the assembly of the instrument, baseline parameter setting, and correction of the instrument before the experiment; thus, large-scale upgrading of the process is impossible. Lan et al. (2022) synthesized a fluorescent probe. Bener et al. (Bener et al., 2020) developed an optical sensor suitable for determining sulfite content in complex samples. However, these methods are too complicated; the synthesis process of the two methods is very complex and difficult to master. The professional quality of the synthesizers is high, and a skilled technician is required to perform the operation. Consequently, most people cannot repeat the experiment.

Based on the findings, it is evident that the use of the printing paper as a flexible SERS substrate showed good sensitivity for the detected sample. The linear correlation of the standard curve indicated that accurate quantitative analysis could be carried out, thus indicating that it could be used for quantitative analysis of sodium sulfite as the target object.

4. Conclusion

In the present study, a method of preparing a flexible SERS substrate by using an impregnation method and Raman spectroscopy with a portable Raman spectrometer was described for the rapid detection of sulfite in foods. This method has several advantages. First, as a substrate, AgNPs-functionalized printing paper could be cut to any size and shape by the impregnation method and could be bent and overlaid on any irregular sample surface for in situ screening without damaging the raw material and maintaining the number of "hotspot" on the substrate. Second, as a SERS substrate, AgNP@FP was cost-effective, easily accessible, and stable, leading to reproducible results. Lastly, compared to other materials, the structure of AgNPs provided the best plasma property and generated a higher SERS EF. The present study also has some limitations. For example, many compounds tested do not exhibit Raman activity. However, some compounds with Raman activity may emit fluorescence at NIR and/or visible laser frequencies. Fluorescence is particularly problematic for Raman spectroscopy, as its signal magnitude is stronger than Raman scattering; this typically results in concealing Raman signals. Therefore, the development of a detection method that combines SERS with other devices in the future will provide greater application prospects.

CRediT authorship contribution statement

Shiyao Wang: Original manuscript preparation. **Yanan Zhao:** Data processing. **Chaofan Zhang:** Data curation. **Shuai Cui**: Data processing. **Yisheng Chen:** Original ideas, Supervision. **Liangxiao Zhang:** Supervision. **Qi Zhang:** Supervision.

Data Availability

No data was used for the research described in the article.

Acknowledgment

This work was supported by Shanxi Province Postdoc Reward [SXBYKY2022001], Shanxi Agricultural University High-Level Talent Project (grant number 2021XG013) and Shanxi Scholarship Council of China (grant number 2021-068).

Declaration of competing interest

We have no known competitive economic interests or personal relationships that might affect the work reported in this article.

Appendix A. Supporting information

Supplementary data associated with this article can be found in the online version at doi:10.1016/j.jfca.2023.105809.

References

Bai, F., Dong, J., Wang, T., Qu, J., Zhang, Z., 2023. Controllable assembly of high sticky and flexibility surface-enhanced Raman scattering substrate for on-site target pesticide residues detection. Food Chem. 405, 134794 https://doi.org/10.1016/j.foodchem.2022.134794.

Bai, X., Xiao, Q., Zhou, L., Tang, Y., He, Y.J.M., 2020. Detection of sulfite dioxide residue on the surface of fresh-cut potato slices using near-infrared hyperspectral imaging system and portable near-infrared spectrometer. Molecules 25 (7), 1651. https://doi.org/10.3390/molecules25071651.

Batool, A., Khan, G.A., Ahmed, W., 2022. Seed-mediated growth of highly concentrated silver nanoparticles on a flexible substrate for applications in SERS-based trace detection. Vib. Spectrosc. 123, 103438 https://doi.org/10.1016/j.vibspec.2022.103438.

Bener, M., Şen, F.B., Apak, R., 2020. Novel pararosaniline based optical sensor for the determination of sulfite in food extracts. Mol. Biomol. Spectrosc. 226, 117643 https://doi.org/10.1016/j.saa.2019.117643.

Carlos, K.S., de Jager, L.S., 2017. Determination of sulfite in food by liquid chromatographytandem mass spectrometry: collaborative study. J. AOAC Int. 100 (6), 1785–1794. https://doi.org/10.5740/jaoacint.17-0033.

Carrascon, V., Ontanon, I., Bueno, M., Ferreira, V., 2017. Gas chromatography-mass spectrometry strategies for the accurate and sensitive speciation of sulfur dioxide in wine. J. Chromatogr. A 1504, 27–34. https://doi.org/10.1016/j.chroma.2017.05.012.

Chen, M., Yang, H., Rong, L., Chen, X., 2016. A gas-diffusion microfluidic paper-based analytical device (μPAD) coupled with portable surface-enhanced Raman scattering (SERS): facile determination of sulphite in wines. Analyst 141 (19), 5511–5519. https://doi.org/10.1039/C6AN00788K.

Chen, W.Q., Liu, X.J., Chen, S., Song, X.Z., Kang, J., 2015. A real-time colorimetric and ratiometric fluorescent probe for rapid detection of SO2 derivatives in living cells based on a near-infrared benzopyrylium dye. RSC Adv. 5 (32), 25409–25415. https://doi.org/10.1039/C4RA15067H.

Chen, Y., Wang, X., Yang, X.-F., Zhong, Y., Li, Z., Li, H., 2015. Development of a ratiometric fluorescent probe for sulfite based on a coumarin–benzopyrylium platform. Sens. Actuators B: Chem. 206, 268–275 https://doi.org/10.1016/j.snb.2014.09.052Get rights and content.

Chen, Y., Ge, F., Guang, S., Cai, Z., 2017. Self-assembly of Ag nanoparticles on the woven cotton fabrics as mechanical flexible substrates for surface enhanced Raman scattering. J. Alloy. Compd. 726, 484–489. https://doi.org/10.1016/j.jallcom.2017.07.315.

Cialla, D., März, A., Böhme, R., Theil, F., Weber, K., Schmitt, M., Popp, J., 2012. Surface-enhanced Raman spectroscopy (SERS): progress and trends. Anal. Bioanal. Chem. 403 (1), 27–54 https:// doi.org/ 10.1007/s00216-011-5631-x.

Deng, Z., Chen, X.X., Wang, Y.R., Fang, E.H., Zhang, Z.G., Chen, X., 2015. Headspace thin-film microextraction coupled with surface-enhanced raman scattering as a facile method for reproducible and specific detection of sulfur dioxide in wine. Anal. Chem. 87 (1), 633–640. https://doi.org/10.1021/ac503341g.

Devarajan, S., Sha, M.S., Geetha, M., Alahmad, J.K., Shaikh, M.S.T., Muthusamy, S., Kushwah, K.K., Sadasivuni, Kk, 2023. A paper-based colourimetric sensor for sodium sulfite detection in beverages. J. Food Meas. Charact. 17, 3973–3979. https://doi.org/10.1007/s11694-023-01929-1.

Dong, J., Cai, L., Wang, S., Wang, Y., Chen, X.J.A.L., 2019. Determination of sulfite in botanical medicine using headspace thin-film microextraction and surface enhanced Raman spectrometry. Anal. Lett. 52 (8), 1236–1246. https://doi.org/10.1080/00032719.2018.1529183.

Fang, H., Zhang, X., Zhang, S.J., Liu, L., Zhao, Y.M., Xu, H.J., 2015. Ultrasensitive and quantitative detection of paraquat on fruits skins via surface-enhanced Raman spectroscopy. Sens. Actuators B: Chem. 213, 452–456. https://doi.org/10.1016/j.snb.2015.02.121.

Gao, W., Xu, J., Cheng, C., Qiu, S., Jiang, S., 2020. Rapid and highly sensitive SERS detection of fungicide based on flexible “wash free” metallic textile. Appl. Surf. Sci. 512, 144693 https://doi.org/10.1016/j.apsusc.2019.144693.

Gonçalves, S., Alves, V.R., Pérez, S.O., Ferreira, M., Daguer, H., de Oliveira, M.A.L., Micke, G.A., Vitali, L., 2020. Rapid method for the determination of citrate, phosphate and sulfite in seafood by capillary zone electrophoresis. Food Chem. 321, 126705 https://doi.org/10.1016/j.foodchem.2020.126705.

Han, X., Zhu, F., Chen, L., Wu, H., Wang, T., Chen, K., 2020. Mechanism analysis of toxicity of sodium sulfite to human hepatocytes L02. Mol. Cell. Biochem. 473 (1–2), 25–37. https://doi.org/10.1007/s11010-020-03805-8.

Huang, T., Hou, Z., Xu, Q., Huang, L., Li, C., Zhou, Y., 2017. Polymer vesicle sensor for visual and sensitive detection of so2 in water. Langmuir 33 (1), 340–346. https://doi.org/10.1021/acs.langmuir.6b03869.

Irwin, S.V., Fisher, P., Graham, E., Malek, A., Robidoux, A., 2017. Sulfites inhibit the growth of f our species of beneficial gut bacteria at concentrations regarded as safe for food. Plos One 12 (10), 742–745. https://doi.org/10.1371/journal.pone.0186629.

Khan, G.A., Demirtaş, O.Ö., Bek, A., Bhatti, A.S., Ahmed, W., 2022. Facile fabrication of Au-Ag alloy nanoparticles on filter paper: application in SERS based swab detection and multiplexing. Vib. Spectrosc. 120, 103359 https://doi.org/10.1016/j.vibspec.2022.103359.

Lajin, B., Goessler, W., 2019. Exploring the sulfur species in wine by HPLC-ICPMS/MS. Anal. Chim. Acta 1092, 1–8. https://doi.org/10.1016/j.aca.2019.09.074.

Lan, J.-S., Zeng, R.-F., Wang, Y., Zhen, L., Liu, Y., Ho, R.J.Y., Ding, Y., Zhang, T., 2022. All-in-one: Accurate quantification, on-site detection, and bioimaging of sulfite using a colorimetric and ratiometric fluorescent probe in vitro and in vivo. J. Hazard. Mater. 424, 127229 https://doi.org/10.1016/j.jhazmat.2021.127229.

Lee, P.C., Meisel, D., 1982. Adsorption and surface-enhanced Raman of dyes on silver and gold sols. J. Phys. Chem. 86 (17), 3391–3395. https://doi.org/10.1021/j100214a025.

Lester, M.R., 1995. Sulfite sensitivity: significance in human health. J. Am. Coll. Nutr. 14 (3), 229–232. https://doi.org/10.1080/07315724.1995.10718500.

Li, C., Song, M., Wu, S., Wang, Z., Duan, N., 2022a. Selection of aptamer targeting levamisole and development of a colorimetric and SERS dual-mode aptasensor based on AuNPs/Cu-TCPP(Fe) nanosheets. Talanta 251, 123739. https://doi.org/10.1016/j.talanta.2022.123739.

Li, T., Chen, X., Wang, K., Hu, Z., 2022. Small-molecule fluorescent probe for detection of sulfite. Pharmaceuticals 15 (11), 1326. https://doi.org/10.3390/ph15111326.

Lin, Z., He, L., 2019. Recent advance in SERS techniques for food safety and quality analysis: a brief review. Curr. Opin. Food Sci. 28, *82–87* https://doi.org/10.1016/j.cofs.2019.10.001Get rights and content.

Liu, M., Lu, J., Chen, Y., Shi, X., Li, Y., Yang, S., Yu, J., Guan, S., 2021. Sodium sulfite-induced mast cell pyroptosis and degranulation. J. Agric. Food Chem. 69 (27), 7755–7764. https://doi.org/10.1021/acs.jafc.1c02436.

Liu, S., Guo, J., Hinestroza, J.-P., Kong, X., Yu, Q., 2021. Fabrication of plasmonic absorbent cotton as a SERS substrate for adsorption and detection of harmful ingredients in food. Microchem. J. 170, 106662 https://doi.org/10.1016/j.microc.2021.106662.

Mandal, P., Tewari, B.S., 2022. Progress in surface enhanced Raman scattering molecular sensing: a review. Surf. Interfaces 28, 101655. https://doi.org/10.1016/j.surfin.2021.101655.

Manikandan, V.S., Liu, Z., Chen, A., 2018. Simultaneous detection of hydrazine, sulfite, and nitrite based on a nanoporous gold microelectrode. J. Electroanal. Chem. 819, 524–532. https://doi.org/10.1016/j.jelechem.2018.02.004.

Oshimo, M., Nakashima, F., Kai, K., Matsui, H., Shibata, T., Akagawa, M., 2021. Sodium sulfite causes gastric mucosal cell death by inducing oxidative stress. Free Radic. Res. 55 (6), 731–743. https://doi.org/10.1080/10715762.2021.1937.

Pang, S., Yang, T., He, L., 2016. Review of surface enhanced Raman spectroscopic (SERS) detection of synthetic chemical pesticides. TrAC Trends Anal. Chem. 85, 73–82. https://doi.org/10.1016/j.trac.2016.06.017.

Qu, D., Gu, Y., Feng, L., Han, J., 2017. High Content Analysis technology for evaluating the joint toxicity of sunset yellow and sodium sulfite in vitro. Food Chem. 233, 135–143. https://doi.org/10.1016/j.foodchem.2017.04.102.

Robbins, K.S., Shah, R., MacMahon, S., de Jager, L.S., 2015. Development of a liquid chromatography–tandem mass spectrometry method for the determination of sulfite in food. J. Agric. Food Chem. 63 (21), 5126–5132. https://doi.org/10.1021/jf505525z.

Shang, Y., Chen, X., Liu, W., Tan, P., Chen, H., Wu, L., Ma, C., Xiong, X., Pan, J., 2017. Photocorrosion inhibition and high-efficiency photoactivity of porous g-C3N4/Ag2CrO4 composites by simple microemulsion-assisted co-precipitation method. Appl. Catal. B: Environ. 204, 78–88. https://doi.org/10.1016/j.apcatb.2016.11.025.

Shariat, M., 2023. Plasma jet printing of silver nanoparticles on polyester fabric as a surface-enhanced Raman scattering substrate. Optik 277, 170698. https://doi.org/10.1016/j.ijleo.2023.170698.

Shi, Y., Liu, W., Chen, C., 2016. Two-step centrifugation method for subpicomolar surface-enhanced Raman scattering detection. Anal. Chem. 88 (9), 5009–5015. https://doi.org/10.1021/acs.analchem.6b01194.

Tian, X., Zhai, P., Guo, J., Yu, Q., Xu, L., Yu, X., Wang, R., Kong, X., 2021. Fabrication of plasmonic cotton gauze-Ag composite as versatile SERS substrate for detection of pesticides residue. Spectrochim. Acta Part A: Mol. Biomol. Spectrosc. 257, 119766 https://doi.org/10.1016/j.saa.2021.119766.

Urupina, D., Gaudion, V., Romanias, M.N., Verriele, M., Thevenet, F., 2020. Method development and validation for the determination of sulfites and sulfates on the surface of mineral atmospheric samples using reverse-phase liquid chromatography. Talanta 219, 121318. https://doi.org/10.1016/j.talanta.2020.121318.

Wang, L., Chen, Y., 2020. A reaction-triggered luminescent Ce(4+)/Tb(3+) MOF probe for the detection of SO(2) and its derivatives. Chem. Commun. 56 (51), 6965–6968. https://doi.org/10.1039/C9CC09900J.

Wang, X., Cao, H., Guan, X.L., Long, L.H., Hu, Z.L., Ni, L., Wang, F., Chen, J.G., Wu, P.F., 2016. Sulfite triggers sustained calcium overload in cultured cortical neurons via a redox-dependent mechanism. Toxicol. Lett. 258, 237–248. https://doi.org/10.1016/j.toxlet.2016.06.009.

Weng, G., Feng, Y., Zhao, J., Li, J., Zhu, J., Zhao, J., 2019. Size dependent SERS activity of Ag triangular nanoplates on different substrates: glass vs paper. Appl. Surf. Sci. 478, 275–283. https://doi.org/10.1016/j.apsusc.2019.01.142.

Yang, Y., Yan, W., Guo, C., Zhang, J., Yu, L., Zhang, G., Wang, X., Fang, G., Sun, D., 2020. Magnetic molecularly imprinted electrochemical sensors: a review. Anal. Chim. Acta 1106, 1–21. https://doi.org/10.1016/j.aca.2020.01.044.

Yang, Y., Shi, Z., Chang, Y., Wang, X., Yu, L., Guo, C., Zhang, J., Bai, B., Sun, D., Fan, S., 2021a. Surface molecularly imprinted magnetic MOFs: a novel platform coupled with magneto electrode for high throughput electrochemical sensing analysis of oxytetracycline in foods. Food Chem. 363, 130337 https://doi.org/10.1016/j.foodchem.2021.130337.

Yang, Y., Yan, W., Wang, X., Yu, L., Zhang, J., Bai, B., Guo, C., Fan, S.J.B., Bioelectronics, 2021. Development of a molecularly imprinted photoelectrochemical sensing

platform based on NH2-MIL-125 (Ti)–TiO2 composite for the sensitive and selective determination of oxtetracycline. Biosens. Bioelectron. 177, 113000 https://doi.org/10.1016/j.bios.2021.113000.

Yang, Y., Yang, L., Ma, Y., Wang, X., Zhang, J., Bai, B., Yu, L., Guo, C., Zhang, F., Qin, S.J. F.C., 2022. A novel metal–organic frameworks composite-based label-free point-of-care quartz crystal microbalance aptasensing platform for tetracycline detection. Food Chem. 392, 133302 https://doi.org/10.1016/j.foodchem.2022.133302Get rights and content.

Yang, Y., Shi, Z., Wang, X., Bai, B., Qin, S., Li, J., Jing, X., Tian, Y., Fang, G.J.F.C., 2022. Portable and on-site electrochemical sensor based on surface molecularly imprinted magnetic covalent organic framework for the rapid detection of tetracycline in food. Food Chem. 395, 133532 https://doi.org/10.1016/j.foodchem.2022.133532.

Yang, Y., Wei, H., Wang, X., Sun, D., Yu, L., Bai, B., Jing, X., Qin, S., Qian, H.J.B., Bioelectronics, 2023. MOF/COF heterostructure hybrid composite-based molecularly imprinted photoelectrochemical sensing platform for determination of dibutyl phthalate: a further expansion for MOF/COF application. Biosens. Bioelectron. 223, 115017 https://doi.org/10.1016/j.bios.2022.115017.

Yang, Z., Chen, G., Ma, C., Gu, J., Zhu, C., Li, L., Gao, H., 2023. Magnetic Fe3O4@COF@Ag SERS substrate combined with machine learning algorithms for detection of three quinolone antibiotics: ciprofloxacin, norfloxacin and levofloxacin. Talanta 263, 124725. https://doi.org/10.1016/j.talanta.2023.124725.

Yao, G., Yue, H., Yun, Y., Sang, N., 2015. Chronic SO2 inhalation above environmental standard impairs neuronal behavior and represses glutamate receptor gene expression and memory-related kinase activation via neuroinflammation in rats. Environ. Res. 137, 85–93. https://doi.org/10.1016/j.envres.2014.11.012.

Yao, G.Y., Yun, Y., Sang, N., 2016. Differential effects between one week and four weeks exposure to same mass of SO2 on synaptic plasticity in rat hippocampus. Environ. Toxicol. 31 (7), 820–829. https://doi.org/10.1002/tox.22093.

Zhang, C., You, T., Yang, N., Gao, Y., Jiang, L., Yin, P., 2019. Hydrophobic paper-based SERS platform for direct-droplet quantitative determination of melamine. Food Chem. 287, 363–368. https://doi.org/10.1016/j.foodchem.2019.02.094.

Zhang, Y., Guan, L., Yu, H., Yan, Y., Du, L., Liu, Y., Sun, M., Huang, D., Wang, S., 2016. Reversible fluorescent probe for selective detection and cell imaging of oxidative stress indicator bisulfite. Anal. Chem. 88 (8), 4426–4431. https://doi.org/10.1021/acs.analchem.6b00061.

Zheng, W., Tian, W., Liu, X., Zhang, Q., Zong, C., Lai, J.-P., Zhao, W., 2021. In situ photochemical deposition of Ag nanoparticles on polyester fiber membranes as flexible SERS substrates for sensitive detection of sodium saccharin in soft drinks. Microchem. J. 164, 106003 https://doi.org/10.1016/j.microc.2021.106003.